Estimating photosynthetic ^{13}C discrimination in terrestrial CO_2 exchange from canopy to regional scales

Chun-Ta Lai,[1] James R. Ehleringer,[1] Pieter Tans,[2] Steven C. Wofsy,[3] Shawn P. Urbanski,[3] and David Y. Hollinger[4]

Received 11 September 2003; revised 12 January 2004; accepted 28 January 2004; published 18 March 2004.

[1] We determined $\delta^{13}C$ values associated with canopy gross and net CO_2 fluxes from four U.S. sites sampled between 2001 and 2002. Annual mean, flux-weighted $\delta^{13}C$ values of net ecosystem CO_2 exchange (NEE) were estimated for four contrasting ecosystems (three forests and one grassland) by analyzing daytime flask measurements collected at the top of canopies. Combining $\delta^{13}C$ values associated with respiratory and net (respiration minus photosynthesis) fluxes, we demonstrate a method for estimating whole-canopy photosynthetic discrimination against ^{13}C (Δ_A) in terrestrial ecosystems directly from field measurements. This experimental approach offers the possibility of examining interannual variability in Δ_A from ecosystem $\delta^{13}C$ measurements. Our estimated $\delta^{13}C$ values associated with photosynthetic fluxes are in agreement with those measured from foliar organic matter for C_3 forests, and are within the range bounded by C_3 and C_4 grasses in a tallgrass prairie. The $\delta^{13}C$ associated with NEE fluxes at our C_3 forest sites ranges between -27.1 ± 2.7 and -28.3 ± 2.5‰, and is -22.6 ± 4.0‰ at the prairie site. These estimates differ from a previous study, particularly for C_3 ecosystems at comparable latitudes. Sensitivity analyses indicate that our estimates of $\delta^{13}C$ values of net CO_2 fluxes are robust with respect to measurement errors, but can vary depending on the selection of background atmospheric values. Other factors (e.g., drought and sampling footprint) that might have influenced our $\delta^{13}C$ measurements and calculations of Δ_A are also discussed. Our measurement-based analyses are particularly useful when both latitudinal and longitudinal variations in Δ_A are to be considered in the global inversion modeling studies. *INDEX TERMS:* 0315 Atmospheric Composition and Structure: Biosphere/atmosphere interactions; 0322 Atmospheric Composition and Structure: Constituent sources and sinks; 1040 Geochemistry: Isotopic composition/chemistry; 1615 Global Change: Biogeochemical processes (4805); *KEYWORDS:* ^{13}C discrimination, biosphere-atmosphere CO_2 exchange, carbon isotopes, CO_2 mixing ratios, isotopic air sampling, isotopic disequilibrium

Citation: Lai, C.-T., J. R. Ehleringer, P. Tans, S. C. Wofsy, S. P. Urbanski, and D. Y. Hollinger (2004), Estimating photosynthetic ^{13}C discrimination in terrestrial CO_2 exchange from canopy to regional scales, *Global Biogeochem. Cycles*, *18*, GB1041, doi:10.1029/2003GB002148.

1. Introduction

[2] Measurements of $^{13}C/^{12}C$ in the atmosphere provide useful information to study the overall balance of surface CO_2 fluxes. At the global scale, $\delta^{13}C$ values are used to partition terrestrial and oceanic sinks of atmospheric CO_2 [*Keeling et al.*, 1989, 1995, 1996, 2001; *Tans et al.*, 1993; *Enting et al.*, 1995; *Francey et al.*, 1995; *Fung et al.*, 1997; *Ciais et al.*, 1999; *Rayner et al.*, 1999; *Battle et al.*, 2000]. At the ecosystem scale, these signatures can be used to partition net CO_2 fluxes into photosynthetic and respiratory compartments [*Yakir and Wang*, 1996; *Bowling et al.*, 2001a, 2003; *Ogée et al.*, 2003; *Lai et al.*, 2003]. Distinct isotopic signatures between sources and sinks are necessary in order to utilize $\delta^{13}C$ values to partition net surface fluxes. For instance, oceans discriminate roughly 10 times less against ^{13}C than most terrestrial vegetation, which has allowed the isotopic signal in atmospheric CO_2 to be a powerful tracer for constraining carbon budget analyses.

[3] Plants discriminate against ^{13}C during CO_2 uptake [*Farquhar et al.*, 1989], resulting in an enriched ^{13}C signal for the CO_2 remaining in the atmosphere. On the other hand, respiration releases ^{13}C-depleted CO_2 to the atmosphere. These distinct ^{13}C signatures are useful tracers to characterize gross CO_2 fluxes at the canopy-atmosphere

[1]Department of Biology, University of Utah, Salt Lake City, Utah, USA.
[2]National Oceanic and Atmospheric Administration/Climate Monitoring and Diagnostics Laboratory, Boulder, Colorado, USA.
[3]Division of Engineering and Applied Science and Department of Earth and Planetary Science, Harvard University, Cambridge, Massachusetts, USA.
[4]USDA Forest Service, Northeastern Research Station, Durham, New Hampshire, USA.

Copyright 2004 by the American Geophysical Union.
0886-6236/04/2003GB002148$12.00

interface. During the day, the observed CO_2 mixing ratio and ^{13}C composition of CO_2 ($\delta^{13}CO_2$) reflect the relative strengths of photosynthesis and respiration, while at night, measurements reflect an integrated estimate of all respired components. If gross CO_2 fluxes are independently determined, it is possible to estimate ^{13}C composition of gross primary production fluxes ($\delta^{13}C_A$). Quantifying $\delta^{13}C_A$ is important for accurate inversions of CO_2 source and sink distributions [*Lloyd and Farquhar*, 1994; *Ciais et al.*, 1995; *Fung et al.*, 1997; *Randerson et al.*, 2002; *Scholze et al.*, 2003].

[4] Current global inverse models assuming constant terrestrial discrimination against ^{13}C (Δ_A) may have overestimated the interannual variability of oceanic and terrestrial fluxes required for global CO_2 budget closure [*Randerson et al.*, 2002; *Scholze et al.*, 2003]. Difficulties in direct measurement of $\delta^{13}C_A$ have led to alternatives for examining the seasonality in $\delta^{13}C_A$ [*Conte and Weber*, 2002]. A common approach is to record ^{13}C signatures during respiration to infer what happens during photosynthesis. Recent studies suggest that respired CO_2 consists of a large portion of recently fixed carbon substrates [*Högberg et al.*, 2001; *Ekblad and Högberg*, 2001; *Bowling et al.*, 2002], indicating a rapid recycling of recent photosynthesis into current respiration. Assuming constant background CO_2 mixing ratio and $\delta^{13}CO_2$ [*Miller et al.*, 2003], a two-source mixing model can be used to describe the carbon isotopic composition of respired CO_2 sources ($\delta^{13}C_R$) [*Keeling*, 1958],

$$\delta^{13}C_m = \frac{C_{bg}}{C_m}\left(\delta^{13}C_{bg} - \delta^{13}C_R\right) + \delta^{13}C_R, \qquad (1)$$

where C represents mixing ratios of CO_2, and subscripts m and bg represent measurements collected within the canopy boundary layer and the background atmosphere, respectively. For canopy air sampling, the assumption of constant background mixing ratio and $\delta^{13}C$ of atmospheric CO_2 is satisfied on a daily basis, so that flasks collected over one night can be used to estimate isotopic composition of respired sources using a "Keeling-plot" approach [*Flanagan and Ehleringer*, 1998].

[5] Significant seasonal cycles in $\delta^{13}C_R$ were observed at tower-based experiments in North America (C.-T. Lai et al., Imbalance of $^{13}CO_2$ fluxes between photosynthesis and respiration in North American temperate forest biomes, submitted to *Global Change Biology*, 2004) (hereinafter referred to as Lai et al., submitted manuscript, 2004) and Europe (D. Hemming et al., unpublished data, 2004). Seasonal variations in $\delta^{13}C_R$ reflect temporal changes in $\delta^{13}C_A$ and may induce large isotopic forcing, altering the atmospheric ^{13}C budget. On an annual timescale, however, it is less clear how $\delta^{13}C_A$, $\delta^{13}C_R$, and gross fluxes would covary and create a significant isotopic disequilibrium [*Ciais et al.*, 1995; *Fung et al.*, 1997; *Randerson et al.*, 2002].

[6] Interpreting atmospheric $\delta^{13}CO_2$ data is complicated by differential fractionations associated with the two major photosynthetic pathways. C_4 photosynthesis discriminates less against ^{13}C than C_3 photosynthesis, and its discrimination value approaches that of oceans. C_4 plants are concentrated in subtropical and tropical regions with ample precipitation and high light environment [*Ehleringer et al.*, 1997; *Sage et al.*, 1999; *Still et al.*, 2003]. Global modeling studies which incorporate mechanistic models predict latitudinal gradients of mean terrestrial discrimination in the Northern Hemisphere associated with differential C_3-C_4 plant distributions [*Lloyd and Farquhar*, 1994; *Fung et al.*, 1997; *Still et al.*, 2003] (also S. Suits et al., Simulation of carbon isotope discrimination of the terrestrial biosphere, submitted to *Global Biogeochemical Cycles*, 2003) (hereinafter referred to as Suits et al., submitted manuscript, 2003). Longitudinal variations in vegetation types associated with changes in precipitation will also influence ecosystem-scale $\delta^{13}C$ values, especially when compared with model calculations. Field observations are important to characterize effects of temperature and water availability on $\delta^{13}C_R$. Direct measurements can also define the bounds of modeled $\delta^{13}C_A$ for regions of a dominant vegetation type within a latitudinal band.

[7] In this study, we use nearly 2 years of CO_2 mixing ratio and $\delta^{13}CO_2$ measurements collected in four terrestrial ecosystems in the United States, and link these data with large-scale atmospheric patterns to investigate $\delta^{13}C$ signatures associated with biospheric fluxes. We investigate $\delta^{13}C$ values in a deciduous and two coniferous forests as well as in a C_4-dominated grassland. No previous study has provided both daytime and nighttime $\delta^{13}C$ measurements at timescales as fine as the current study or in such diversified ecosystems. Values of $\delta^{13}C_R$ were measured weekly during the growing season for all four sites; using weekly data, $\delta^{13}C$ values associated with net CO_2 fluxes were estimated on an annual basis. In combination with eddy covariance flux measurements, we demonstrate a method for estimating a whole-canopy photosynthetic discrimination against ^{13}C from direct measurements. Errors associated with our experimental approach are estimated, and factors that might influence our interpretation of canopy $\delta^{13}C$ measurements are also addressed. Frequent, long-term stable isotope measurements in terrestrial ecosystems should improve the accuracy of global inversion analyses for separating oceanic and terrestrial uptakes of anthropogenic CO_2 inputs.

2. Methods

[8] CO_2 mixing ratios and $\delta^{13}CO_2$ over a terrestrial canopy are mainly affected by CO_2 contributions from biological activities (C_{bio}) and fossil fuel combustion (C_{ff}), added to some background value of CO_2 mixing ratio (C_{bg}) with an associated $\delta^{13}C$ content ($\delta^{13}C_{bg}$). Mass balance equations can be written for the observed mixing ratio and $\delta^{13}C$ of CO_2 over plant canopies as

$$C_m = C_{bg} + C_{bio} + C_{ff} \qquad (2)$$

$$\delta^{13}C_m C_m = \delta^{13}C_{bg}C_{bg} + \delta^{13}C_{bio}C_{bio} + \delta^{13}C_{ff}C_{ff}, \qquad (3)$$

where $\delta^{13}C_{bio}$ and $\delta^{13}C_{ff}$ represent carbon isotope ratios associated with biological activities and fossil fuel combustion, respectively. As with CO_2, each $\delta^{13}C$ value in equation (3) represents a flux-weighted quantity of respective processes. For instance, $\delta^{13}C_{bio}$ characterizes

the carbon isotope composition of net CO_2 fluxes exchanged between the atmosphere and a plant canopy, and represents the isotopic balance between photosynthesis and respiration. Notice that in equation (3), CO_2 exchange between the atmosphere and oceans is relatively small at continental sites and can be ignored [*Bakwin et al.*, 1998; *Miller et al.*, 2003].

[9] *Bakwin et al.* [1998] and *Potosnak et al.* [1999] showed during the growing season that biological activities dominate CO_2 mixing ratio and $\delta^{13}CO_2$ measurements in terrestrial ecosystems, such that $C_{ff} \ll C_{bio}$. Rearranging equations (2) and (3), we arrive at the following equation which effectively describes what happens during the growing season:

$$\left(\delta^{13}C_m C_m - \delta^{13}C_{bg}C_{bg}\right) = \delta^{13}C_{bio}\left(C_m - C_{bg}\right). \quad (4)$$

Equation (4) is derived from the same mass balance equations of $^{12}CO_2$ and $^{13}CO_2$ that are used to derive the Keeling relation (equation (1)). However, this form, originally derived by P. Tans, has an advantage when analyzing a time series of air samples collected over multiple seasons or years, where the assumption of constant background CO_2 mixing ratio and $\delta^{13}CO_2$ is violated [*Miller et al.*, 2003; *Miller and Tans*, 2003]. Through a linear regression analysis with $X = C_m - C_{bg}$ and $Y = \delta^{13}C_m C_m - \delta^{13}C_{bg}C_{bg}$, we obtain $\delta^{13}C_{bio}$ as the slope of the regression. Because measurement errors occur in both dependent and independent variables, a geometric mean regression (Model II) is required for this analysis [*Pataki et al.*, 2003a]. Notice that equation (4) has an intercept of zero. Since geometric mean regression should not be forced through the origin, we can justify the appropriateness of this model to the observed data by testing statistical significance of the intercept. If an intercept is statistically different from zero, it suggests that equation (4) may not be an appropriate model to explain the variance observed in the data. Therefore the assumption $C_{ff} \ll C_{bio}$ might have been violated.

[10] When C_{ff} becomes significant relative to the other terms, all terms in equations (2) and (3) need to be considered in order to estimate $\delta^{13}C_{bio}$. The fraction of observed CO_2 derived from fossil fuel combustion can be estimated by concurrent measurements of carbon monoxide (CO) [*Potosnak et al.*, 1999; *Bakwin et al.*, 1998], $\delta^{14}C$ [*Meijer et al.*, 1997; *Takahashi et al.*, 2001], or $\delta^{18}O$ [*Florkowski et al.*, 1998; *Pataki et al.*, 2003b]. *Bakwin et al.* [1998] and *Miller et al.* [2003] found no significant contribution of fossil fuel combustion to the overall CO_2 concentration during summer months at many continental sites. In this study, we will assume $C_{ff} \ll C_{bio}$ and use the simplified model to estimate $\delta^{13}C_{bio}$, but examine the regressed intercept to justify our assumption $C_{ff} \ll C_{bio}$ at each station.

[11] To use equation (4) for estimating $\delta^{13}C_{bio}$, C_{bg} and $\delta^{13}C_{bg}$ need to be quantified independently. Regional values of background air required to estimate fluxes of trace gases emitted from land or ocean surfaces are ill-defined and difficult to quantify. From a mass balance perspective, background air represents the starting point of a mixing process that includes physical transport, biological production, and chemical reaction of trace gases of interest. For passive scalars like CO_2 at a local station, the background CO_2 mixing ratio and $\delta^{13}CO_2$ incorporate CO_2 exchange with the land biosphere, oceans, and fossil fuel inputs at some timescale of atmospheric transport. While the concept of background air is intuitive, it is not very clear how to quantify this imaginary starting point given the dynamics of atmospheric boundary layer phenomena. Airborne experiments can be used to collect air samples in the free atmosphere, but are expensive and are still subject to weather conditions. Alternatively, measurements in the marine boundary layer can be used as a proxy for background air. *Potosnak et al.* [1999] demonstrated good correlations between air measurements collected at a marine station and background air defined by local CO and CO_2 measurements at the Harvard Forest. In this study, we use the Globalview reference marine boundary layer (MBL) matrix from the NOAA/CMDL network to extract MBL values of CO_2 mixing ratio and $\delta^{13}CO_2$ at the same latitude as each of our four local stations for specific values of C_{bg} and $\delta^{13}C_{bg}$. Procedures for deriving C_{bg} and $\delta^{13}C_{bg}$ are described in section 2.2.

2.1. Study Sites

[12] The atmospheric sampling measurements occurred in four contrasting terrestrial biomes: a western coniferous forest (Wind River Canopy Crane Research Facility (WRCCRF), WA, 45°49′N, 121°58′W), a C_4-dominated tallgrass prairie (Rannell Flint Hills Prairie, KS, 39°07′N, 94°21′W), a temperate deciduous forest (Harvard Forest, MA, 42°32′N, 72°11′W), and an eastern coniferous forest (Howland Forest, ME, 45°15′N, 68°45′W). These four sites comprise major vegetation types in the United States and are sites within the AmeriFlux network. Coincidentally, these four sites are also located in the latitudinal band with the largest latitudinal gradient in ^{13}C discrimination predicted by an earlier global carbon cycle modeling study [*Fung et al.*, 1997].

2.2. Defining C_{bg} and $\delta^{13}C_{bg}$

[13] Defining background values for trace gases exchanged between the atmosphere and the biosphere is not trivial. Ideally, regional background CO_2 mixing ratio and $\delta^{13}CO_2$ should be measured from the local free atmosphere. Dynamics of the convective boundary layer make it difficult to measure C_{bg} and $\delta^{13}C_{bg}$. Different approaches have been used to characterize background CO_2 mixing ratio and $\delta^{13}CO_2$ [*Bakwin et al.*, 1998; *Potosnak et al.*, 1999; *Miller et al.*, 2003; J. Styles et al., personal communication, 2003; B. Helliker et al., personal communication, 2003], depending on the purpose of each study. For the current analysis, we consider background values that are representative of latitudes where measurement stations are located. Second, background values must represent the mixed global troposphere with minimal local terrestrial effects, such that differences between our local canopy measurements and background air characterize signals of local and regional terrestrial biological activities.

[14] To satisfy these conditions, we use the Globalview reference MBL matrix from NOAA/CMDL's network. The Globalview reference matrix is constructed in weekly intervals with spatial increment of 0.05 sine of latitude from

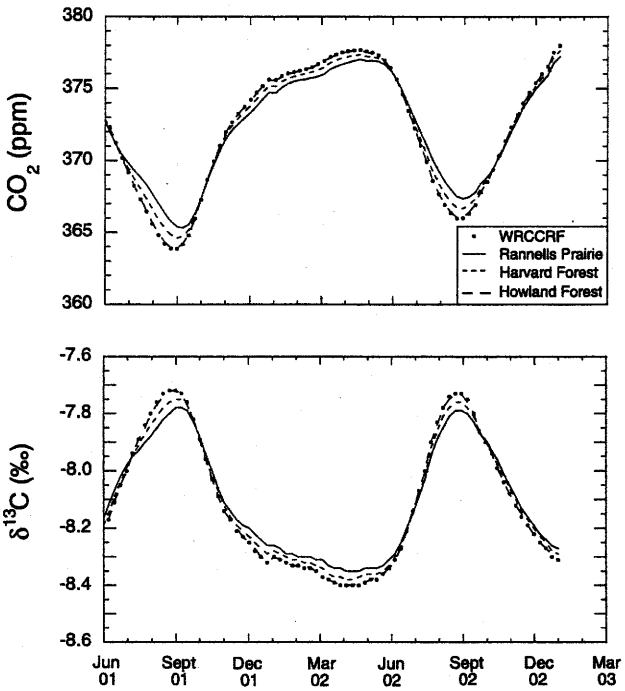

Figure 1. Zonal-mean CO_2 mixing ratio and $\delta^{13}C$ abundance in marine boundary layer (MBL) at latitudes corresponding to our four study sites. Values shown were extracted from Globalview reference MBL matrices within the NOAA/CMDL network.

90°S to 90°N using observations from sampling sites located in the marine boundary layer [*Conway et al.*, 1994; *Francey et al.*, 1995; *Trolier et al.*, 1996], isolated from biospheric carbon sources and sinks [*Globalview-CO2*, 2003; *Masarie and Tans*, 1995]. The Globalview reference matrix allows us to extract a reference MBL time series for any latitude. Methodologies and procedures for constructing the Globalview reference MBL-CO_2 matrix are described by *Globalview-CO2* [2003] and *Masarie and Tans* [1995] and available on the internet via anonymous FTP to ftp://ftp.cmdl.noaa.gov/ccg/co2/GLOBALVIEW/. However, the Globalview reference MBL-$\delta^{13}C$ matrix was specifically constructed, using the same methodologies for the MBL-CO_2 matrix, for the current study and is not available to the general public.

[15] On the basis of the Globalview reference MBL-CO_2 and MBL-$\delta^{13}C$ matrices, we used linear interpolation to extract MBL values of CO_2 mixing ratio and $\delta^{13}CO_2$ for latitudes where our measurement stations are located [*Globalview-CO2*, 2003; *Masarie and Tans*, 1995]. Figure 1 shows these extracted MBL values of CO_2 mixing ratio and $\delta^{13}CO_2$, which were used to represent C_{bg} and $\delta^{13}C_{bg}$, respectively, for each of our local stations.

2.3. Sample Collection and Data Conditioning

[16] The sampling protocol was frequent (weekly) automated collections of C_m and $\delta^{13}C_m$ above and inside plant canopies during both daytime and nighttime. This involved an automated air sampling system that collected 15 flasks at weekly intervals during the growing season and at monthly intervals when the vegetation was dormant [*Schauer et al.*, 2003]. Air samples were dried with magnesium perchlorate during collection and stored in 100-mL glass flasks with Teflon stopcocks (Kontes Glass Co., Vineland, N. J.).

[17] As part of the atmospheric sampling scheme, two flasks were collected in the mid-afternoon (usually between 1430 and 1530 local time) from the top of the canopy. From this pair of flasks we calculated an average for the mixing ratio and $\delta^{13}C$ of CO_2 to estimate daytime values at the top of the canopy. Because our measurements were collected within the canopy roughness boundary layer and the two flask members of each pair were collected 15 min apart, they could have been subjected to different local source effects. Measurements were first filtered to remove values where the difference between the two members of a flask pair differed by more than 5 times the isotope analysis precision (0.12‰ for $\delta^{13}C$ VPDB). A flawed flask pair was identified whenever the CO_2 mixing ratio of the two flask members differed by more than 2% of expected value ($\sim$ 7 ppm) based on in situ measurements (S. P. Urbanski et al., unpublished data, 2004). Spurious measurements may have been caused by any of a number of local or analytical effects and were removed from our analyses. Ten percent of the flask samples were excluded on this basis.

[18] Nighttime sampling began an hour after sunset to ensure no effect of photosynthesis on our estimates of $\delta^{13}C_R$. A set of 12 flasks was collected evenly at two heights (0.5 m above ground and mid-canopy) inside the canopy. A data logger governed sampling with a pre-specified range of CO_2 mixing ratio ($\geq$75 ppm) to obtain statistical confidence for constructing weekly Keeling plots during summer months [*Pataki et al.*, 2003a; *Miller and Tans*, 2003]. This expected CO_2 gradient was computed based on measurements of CO_2 mixing ratio in the previous year for the site. Flask collection continues over the course of a night until the specified CO_2 gradient is met. If respired CO_2 does not build up sufficiently (e.g., on a windy night), the system resets itself and repeats the same protocol next day. A minimum CO_2 gradient of 20 ppm was preset in the data logger for winter months when biological activities were much reduced, yielding lower expected CO_2 gradients. The geometric mean regression was used for each Keeling plot to account for measurement errors in both dependent and independent variables [*Sokal and Rohlf*, 1995]. Values of the Keeling intercept ($\delta^{13}C_R$) were rejected if standard errors of the intercept were greater than 3‰; this most often occurred during winter when the CO_2 gradient was small. About 5% of the measured $\delta^{13}C_R$ values were excluded on this basis. Flasks were analyzed for $\delta^{13}CO_2$ at the Stable Isotope Ratio Facility for Environmental Research at the University of Utah using a continuous-flow isotope ratio mass spectrometer system (Precon attached to a Finnigan MAT 252 or Delta S, San Jose, Calif.), and CO_2 mixing ratios were measured with high precision (±0.2 ppm) using a bellows/IRGA system [*Bowling et al.*, 2001b].

2.4. Smooth Curve Fitting

[19] Smooth curves were fitted using the method described by *Thoning and Tans* [1989], where the curve

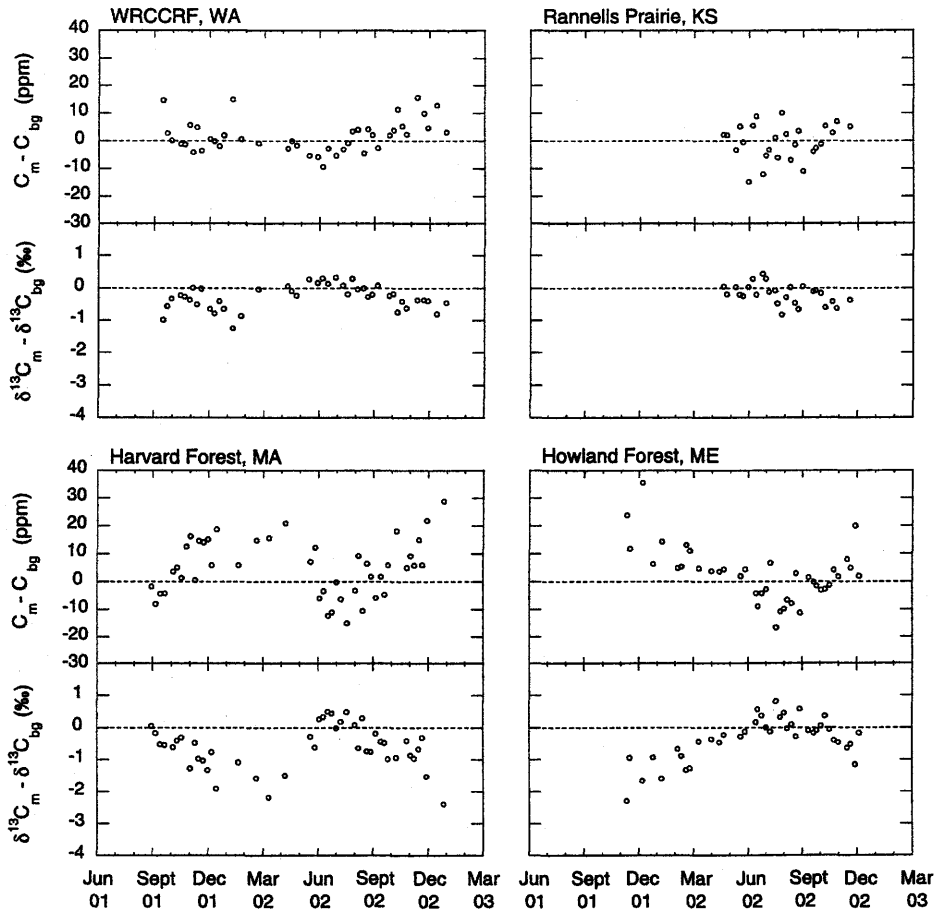

Figure 2. Seasonal variations in the difference between locally measured CO_2 mixing ratio and $\delta^{13}CO_2$ at the top of canopies for all four sites and background values extracted from Globalview reference MBL matrices in the years of 2001 and 2002.

fit function consists of a combination of polynomial and annual harmonics. To alleviate the end-point effect on curve fitting, five projected values were used at each end to guide the curve. Smooth curve fitting to a long record of atmospheric observation requires special attention to detrending [*Thoning and Tans*, 1989]. However, our records of CO_2 mixing ratio and $\delta^{13}CO_2$ were a little longer than 1 year, short enough so that the long-term mean trend was not apparent and had little effect on our smooth curves.

3. Results

3.1. Background CO_2 Mixing Ratio and $\delta^{13}CO_2$

[20] Figure 1 shows the background values of CO_2 mixing ratio and $\delta^{13}CO_2$ for the four study sites, represented by the zonal-mean MBL values at the same latitudes from the Globalview reference matrices. Seasonal patterns resulting from biospheric effects were preserved in the marine boundary layer signals, with greater amplitudes in both CO_2 and $\delta^{13}CO_2$ at higher latitudes. However, these differences were small for the range of latitude associated with our study sites (39°N–45°N). The difference in zonal-mean MBL values does not exceed 2.5 ppm for CO_2 mixing ratio and 0.1‰ for $\delta^{13}CO_2$ among our stations.

3.2. Daytime CO_2 Mixing Ratio and $\delta^{13}CO_2$

[21] Figure 2 shows the difference between locally measured CO_2 mixing ratio and $\delta^{13}CO_2$ at the top of the canopy for all four sites and background MBL values. The strong seasonal pattern shown at the three forest sites clearly demonstrated the biospheric impact on the atmosphere. Between June and September, $\delta^{13}C$ values of canopy air were more enriched while CO_2 mixing ratios were lower than those of background air, suggesting substantial photosynthetic drawdown of CO_2 at these forest sites during these months. During the winter months, locally observed CO_2 values increased and $\delta^{13}CO_2$ decreased at continental sites because of increased impact of fossil fuel inputs, limited photosynthetic CO_2 uptake, and weak convective turbulent mixing. As opposed to the forest sites during summer, observed atmospheric CO_2 mixing ratio and $\delta^{13}CO_2$ in the tallgrass prairie were somewhat confounding, as local $\delta^{13}CO_2$ measurements did not show enriched pattern as the forest sites. In the summer of 2002, Rannells Prairie experienced one of the most severe droughts in decades. In

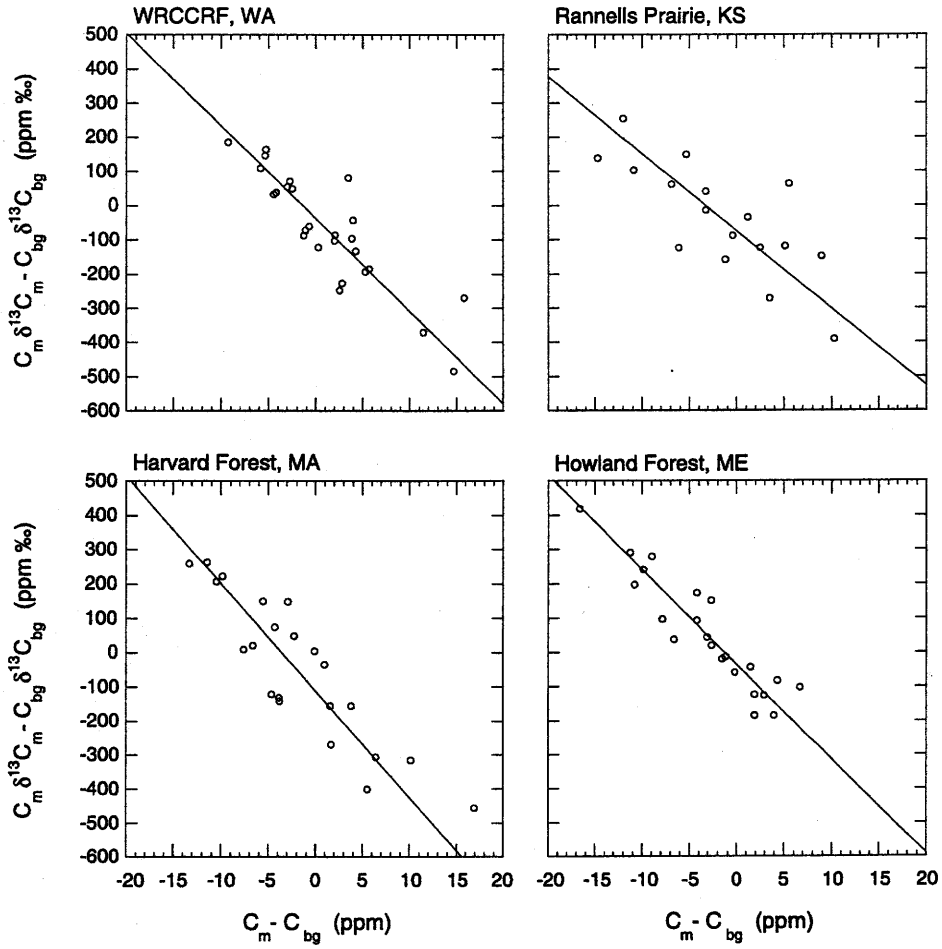

Figure 3. Relationship between deviations of local CO_2 mixing ratio and deviations of the product of CO_2 mixing ratio and $\delta^{13}CO_2$ from background values for all four sites, as described by equation (4).

fact, the drought was so severe that NEE fluxes were positive in most of the afternoon hours for a significant period of time [*Lai et al.*, 2003]. Photosynthetic CO_2 uptakes in this grassland were suppressed due to stomatal closures from the combined effects of low soil water content and high vapor pressure deficits. Soil respiration was also reduced, but to a lesser degree, because of the low soil moisture content [*Lai et al.*, 2003]. These combined effects resulted in a net source of CO_2 in this grassland, creating confounding patterns of mid-afternoon atmospheric CO_2 and $\delta^{13}CO_2$ signals as shown in Figure 2. Also notable in Figure 2 was that at the site closest to the Pacific Ocean (i.e., WRCCRF) the observed mixing ratio and $\delta^{13}C$ of CO_2 were closer to the background air values. As air moved eastward, deviations in local CO_2 and $\delta^{13}CO_2$ from background values became greater, suggestive of an integrating continental effect.

3.3. Estimates of $\delta^{13}C_{bio}$

[22] Flask measurements at continental sites are influenced by both biogenic activities and fossil fuel combustion. Fossil fuel usage increases in winter and the natural gas used in household furnaces has a much depleted ^{13}C composition [*Bakwin et al.*, 1995, 1998; *Pataki et al.*, 2003b]. On the other hand, biogenic activities dominate observed CO_2 in the summer. To satisfy the assumption $C_{ff} \ll C_{bio}$, we applied daytime measurements collected only during the growing season (May to early October) with equation (4) to estimate $\delta^{13}C_{bio}$. Figure 3 shows the relationship between deviations of local C_m and $\delta^{13}C_mC_m$ from background values for all four sites with the Model II regression statistics reported in Table 1. By definition, geometric mean regression is calculated by forcing the line to pass through

Table 1. Results From Model II Regression for a Linear Relationship $Y = \beta_0 + \beta_1 X$, Where $X = C_m - C_{bg}$, $Y = \delta^{13}C_mC_m - \delta^{13}C_{bg}C_{bg}$ and $\beta_1 = \delta^{13}C_{bio}$ (see equation (4))[a]

Site	β_1	$SE_{\beta 1}$	P	β_0	$SE_{\beta 0}$	P	R^2	d.f.
WRCCRF	−27.1	2.7	<0.001	−37.2	16.6	>0.02	0.78	24
Rannells Prairie	−22.6	4.0	<0.001	−74.7	28.7	>0.02	0.59	15
Harvard Forest								
May–October	−31.3	3.5	<0.001	−125.2	23.9	<0.001*	0.77	20
May–July	−28.3	2.5	<0.001	− 59.4	21.8	>0.02	0.93	9
Howland Forest	−27.8	2.4	<0.001	− 36.5	15.7	>0.02	0.86	20

[a]The asterisk indicates intercepts that are significantly different from zero at 98% confidence interval. *P*-values were computed by student-*t* test.

the bivariate mean $\overline{X}$ and $\overline{Y}$ [*Sokal and Rohlf*, 1995]; hence an intercept should always exist. Before applying the simplified model (equation (4)) to explain the variance in C_m and $\delta^{13}C_m$ and for estimating $\delta^{13}C_{bio}$, we tested the significance of the intercept (Table 1). At all but the Harvard Forest site there were insignificant zero intercepts. This meant that equation (4) was appropriate for interpreting the observed variances in CO_2 mixing ratio and $\delta^{13}CO_2$ at WRCCRF, Rannells Prairie, and Howland Forest during the growing season. The slope of this regression gave an estimate of an annual mean, flux-weighted carbon isotopic composition of net CO_2 fluxes ($\delta^{13}C_{bio}$).

[23] The conflict between the simplified model and observed data at the Harvard Forest suggested the assumption ($C_{ff} \ll C_{bio}$) that leads to the derivation of equation (4) be not valid. The sign of the non-zero intercept is actually consistent with a more depleted "constant" contribution, suggesting fossil fuels. The significant influence of fossil fuel combustion on observed CO_2 mixing ratio has been previously reported at the Harvard Forest site using concurrent measurements of CO_2 and CO [*Potosnak et al.*, 1999]. Although the largest anthropogenic impact occurred during winter [*Potosnak et al.*, 1999], there might be sporadic fossil CO_2 inputs in summer depending on wind directions. To alleviate such a potential concern, we examined flasks collected only between May and July when CO_2/CO ratio was lowest (minimal fossil CO_2 impact) [*Potosnak et al.*, 1999]. We reiterate that our goal was to use the simplified model (equation (4)) to estimate $\delta^{13}C_{bio}$ from the observed CO_2 mixing ratio and $\delta^{13}CO_2$. With such a constraint, we reduced the possibility of violating the assumption $C_{ff} \ll C_{bio}$. The intercept became insignificant ($P > 0.02$) if we only use data collected between May and July. The estimated $\delta^{13}C_{bio}$ increased by 3‰ from ~ −31.3‰ to −28.3‰ (see Table 1).

3.4. Nighttime CO_2 Mixing Ratio and $\delta^{13}CO_2$

[24] Measurements of nighttime flasks were analyzed with the "Keeling plot" approach to examine temporal variations in respired isotopic signatures. As shown by Lai et al. (submitted manuscript, 2004), pronounced seasonal changes of $\delta^{13}C_R$ appeared in these C_3 forest ecosystems. That seasonal trend of increasing $\delta^{13}C_R$ correlated with soil moisture availability, reflecting stomatal closure under water stress conditions. We occasionally detected very low $\delta^{13}C_R$ values (−33 to −46‰) at the Harvard Forest during winter. These $\delta^{13}C_R$ values were far too negative to have been derived from this C_3 forest ecosystem and were likely derived from off-site anthropogenic sources. The observed $\delta^{13}C_R$ in the C_4 prairie increased with the progression of the growing season, reflecting the emerging photosynthetic dominance of C_4 species [*Lai et al.*, 2003]. However, isotopic air sampling in heterogeneous ecosystems with more than one photosynthetic pathway requires special attention to sampling footprint [*Still et al.*, 2003; *Lai et al.*, 2003]. This issue will be further discussed later.

3.5. Comparisons of $\delta^{13}C_R$, $\delta^{13}C_{bio}$, and $\delta^{13}C_A$

[25] We have shown estimates of $\delta^{13}C_{bio}$ and $\delta^{13}C_R$ separately using flasks collected during daytime and nighttime. It is important to note that $\delta^{13}C_{bio}$ and $\delta^{13}C_R$ represent ecosystem ^{13}C signatures associated with different fluxes. The $\delta^{13}C_{bio}$ characterizes the ^{13}C signal with respect to the balance between two large gross fluxes: photosynthesis and respiration. The $\delta^{13}C_R$, on the other hand, represents only ecosystem respiration. To put things into a broader perspective, we can calculate a mean $\delta^{13}C_R$ for the growing season ($\overline{\delta^{13}C_R}$) at each site to compare with $\delta^{13}C_{bio}$. This comparison is shown in Table 2, where $\delta^{13}C$ values of leaf organic matter ($\delta^{13}C_{org}$) are also shown. The differences among $\delta^{13}C_{bio}$, $\overline{\delta^{13}C_R}$ and $\delta^{13}C_{org}$ were no greater than 2‰ for each of the C_3 forests. This narrow range implied that the ^{13}C composition of gross primary production fluxes ($\delta^{13}C_A$) was close to that of $\delta^{13}C_{bio}$ or $\delta^{13}C_R$, which was also in agreement with long-term integrated ^{13}C values represented by $\delta^{13}C_{org}$ (Table 2). This agreement was not expected given the observed seasonal variation in $\delta^{13}C_R$.

Table 2. Comparisons of Carbon Isotopic Composition Observed by Three Independent Methods in Four Terrestrial Ecosystems in the United States[a]

Site	$\overline{\delta^{13}C_R}$ (±S.E.), ‰	$\delta^{13}C_{bio}$ (±S.E.), ‰	$\delta^{13}C_{org}$ (±S.E.), ‰
WRCCRF	−26.2 (±0.9)	−27.1 (±2.7)	−25.7 (±0.3)
Rannells Prairie	−15.3 (±0.8)	−22.6 (±4.0)	C_3: −27.9 (±0.5) C_4: −12.0 (±0.3)
Harvard Forest	−26.9 (±0.9)	−28.3 (±2.5)	−27.4 (±0.4)
Howland Forest	−26.5 (±0.9)	−27.8 (±2.4)	−27.3 (±0.5)

[a]Values of $\overline{\delta^{13}C_R}$ are averages for the growing season adopted from Lai et al. (submitted manuscript, 2004), $\delta^{13}C_{bio}$ are regression slopes from equation (4), and $\delta^{13}C_{org}$ represents annual averages of leaf organic matter from sunlit foliage.

[26] We predict that values of $\delta^{13}C_A$ would have been very close to $\overline{\delta^{13}C_R}$ or $\delta^{13}C_{bio}$ between 2001 and 2002 for these C_3 forests. We can use Harvard Forest as an example to carry out a calculation for estimating an annual-mean, canopy-scale Δ_A. From Table 2 we know that $\overline{\delta^{13}C_R}$ = −26.9 and $\delta^{13}C_{bio}$ = −28.3‰. According to *Barford et al.* [2001], the mean GPP, ecosystem respiration (R), and net ecosystem exchange (NEE) fluxes in the 1990s for the Harvard Forest were −13, 11, and −2 Mg C ha^{-1} yr^{-1}, respectively. We can calculate $\delta^{13}C_A$ as

$$\delta^{13}C_{bio} \cdot \mathrm{NEE} = \delta^{13}C_A \cdot \mathrm{GPP} + \overline{\delta^{13}C_R} \cdot R, \qquad (5)$$

which yields $\delta^{13}C_A$ = −27.1‰. Using values of $\delta^{13}C_{bg}$ shown in Figure 1, we calculate mean values of $\delta^{13}C_{bg}$ = −8‰ for the growing season (May–October), with indistinguishable difference among sites. We then calculate photosynthetic discrimination against ^{13}C as $\Delta_A = (-8 - \delta^{13}C_A)/(1 + \delta^{13}C_A/1000)$ = 19.6‰ for this temperate deciduous forest, which is in good agreement with Δ_A values inferred by leaf organic matter (Table 2).

[27] Calculations carried out here only serve to demonstrate an experimental approach for estimating Δ_A. More precise estimates of Δ_A for these four ecosystems require fluxes measured in the same period consistent with our isotope measurements, which is under investigation in a following study (Lai et al., submitted manuscript, 2004). It is useful to quantify errors associated with the experimental approach introduced here. We consider errors for every

measured quantity in equation (5) and propagate errors through calculations of Δ_A. Errors associated with $\delta^{13}C_R$ and $\delta^{13}C_{bio}$ are given in Table 2. If we assume that each flux component can be measured within 5% and propagate errors as the root mean square, values of canopy-scale Δ_A can be estimated within ~7% (or ±1.9‰) for the example shown above.

[28] *Lai et al.* [2003] showed that during the growing season in 2002, measurements of $\delta^{13}C_R$ at Rannells Prairie were occasionally affected by the presence of adjacent C_3 forests and cropland, depending on wind speed and wind direction. Likewise, the estimated $\delta^{13}C_{bio}$ in this prairie indicated a very C_3-like signal during daytime periods (Table 2). Perhaps our daytime observations were compromised by adjacent C_3 cropland, as shown by *Lai et al.* [2003]. This prairie site is located in the center of the Great North American Plains with consistent, high wind speeds. Therefore it is also possible that our daytime flasks represent a regional-scale mixing of C_3/C_4 photosynthesis. *Lai et al.* [2003] showed that summer drought substantially reduced photosynthetic uptake for this tallgrass prairie in 2002. Whether the estimated $\delta^{13}C_{bio}$ value is an anomaly resulting from the severe drought remains a question to be resolved.

[29] It is important to note that the atmospheric $\delta^{13}C$ budget is very sensitive to small changes in global-scale $\delta^{13}C_A$ or $\delta^{13}C_R$. *Randerson et al.* [2002] showed that the magnitude of modeled terrestrial carbon sinks decreased by 0.5 GtC/yr if global-scale $\delta^{13}C_A$ was allowed to vary by only +0.2‰. Year-to-year variability in $\delta^{13}C_A$ is very likely due to vegetation responses to regional drought and climatic events (e.g., El Niño). Measurement-based canopy-scale estimates of Δ_A, like the one derived here, provide opportunities to investigate mechanisms controlling Δ_A, and contribute to constraining modeled results. It is crucial to incorporate knowledge of ecosystem processes into regional-scale models for improving our ability of assessing global distributions of CO_2 sources and sinks.

3.6. Sensitivity Analyses

[30] In calculating an annual-mean, canopy-scale Δ_A using equation (5), $\delta^{13}C_R$, and $\delta^{13}C_{bio}$ need to be known along with gross and net CO_2 fluxes. The Keeling plot approach has been widely adopted, providing reliable estimates of $\delta^{13}C_R$ [*Flanagan et al.*, 1996; *Buchmann et al.*, 1997; *Bowling et al.*, 2002; *Fessenden and Ehleringer*, 2003]. The largest uncertainty regarding the isotopic fluxes appears to be in the estimate of $\delta^{13}C_{bio}$ because of the potential ambiguity in quantifying C_{bg} and $\delta^{13}C_{bg}$. To test the robustness of our estimated $\delta^{13}C_{bio}$, we performed sensitivity analyses with regard to two potential uncertainties: (1) instrument errors and (2) inappropriate description of background air. We caution that a third line of potential errors lies in the possible calibration differences between laboratories for atmospheric CO_2 and $\delta^{13}C$ measurements. On the basis of results of sensitivity tests shown below, we suspect errors associated with calibration differences are small. This issue, however, needs to be investigated upon inter-calibration established in the future.

Table 3a. Sensitivity Analyses for the Estimates of $\delta^{13}C_{bio}(=\beta_1)$, Test A, Considering Measurement Errors From Our Instruments

Site	β_1	$SE_{\beta 1}$	β_0	$SE_{\beta 0}$	P	R^2
WRCCRF	−27.0	2.7	22.9	16.5	>0.05	0.77
Rannells Prairie	−22.5	4.0	−13.7	28.9	>0.05	0.58
Harvard Forest	−28.2	2.5	0.4	22.2	>0.05	0.93
Howland Forest	−27.6	2.4	23.5	15.9	>0.05	0.86

Table 3b. Sensitivity Analyses for the Estimates of $\delta^{13}C_{bio}(=\beta_1)$, Test B, Using Localized Smooth Curves as Background Values[a]

Site	β_1	$SE_{\beta 1}$	β_0	$SE_{\beta 0}$	P	R^2
WRCCRF	−24.0	3.2	1.8	13.0	>0.05	0.61
Rannells Prairie	−20.6	3.1	−9.1	22.4	>0.05	0.68
Harvard Forest	−24.9	1.6	−2.9	11.1	>0.05	0.96
Howland Forest	−27.5	2.5	11.6	11.5	>0.05	0.85

[a]See text.

[31] We carried out two sensitivity tests for the estimate of $\delta^{13}C_{bio}$:

[32] 1. We considered instrument errors: What are the impacts of instrument errors on the estimate of $\delta^{13}C_{bio}$? As shown by *Schauer et al.* [2003], our automated sampler imposed a subtle effect on measured CO_2 mixing ratio and $\delta^{13}CO_2$. The general trend was to artificially increase the CO_2 mixing ratio by as much as 1.5 ppm and decrease the $\delta^{13}CO_2$ value by as much as 0.17‰ over a 5-day period. For this first test, we reduced our observed CO_2 mixing ratios by 1.5 ppm and added 0.17‰ to $\delta^{13}CO_2$ to "adjust" for the maximum-expected instrument artifacts and repeated the analyses for estimating $\delta^{13}C_{bio}$. Table 3a shows that our estimates of $\delta^{13}C_{bio}$ did not significantly differ ($P > 0.05$) at all sites with respect to the maximum potential instrument-induced artifacts.

[33] 2. We used localized smooth curves for C_{bg} and $\delta^{13}C_{bg}$: In this second test we considered a different approach to estimate C_{bg} and $\delta^{13}C_{bg}$, then re-evaluated its impact on the estimate of $\delta^{13}C_{bio}$. *Bakwin et al.* [1998] and *Miller et al.* [2003] suggested using smooth curves fitted to local measurements to represent regionally averaged background values, then adopting deviations of individual observations from smooth curves as "signals" of surface CO_2 exchange. For this sensitivity test, we used smooth curves fitted to our daytime flask measurements collected above canopies to represent C_{bg} and $\delta^{13}C_{bg}$, and re-calculated $\delta^{13}C_{bio}$. Table 3b shows that when C_{bg} and $\delta^{13}C_{bg}$ were quantified by this approach, the estimated $\delta^{13}C_{bio}$ increased by 2–3‰ for all sites but Howland Forest. Interestingly, the more positive values of $\delta^{13}C_{bio}$ yielded by this approach were in better agreement with those reported by *Bakwin et al.* [1998] and *Miller et al.* [2003]. We reiterate that the only difference in our calculation for this test was to replace C_{bg} and $\delta^{13}C_{bg}$ extracted from Global-view MBL matrices by values of smooth curves fitted to local flask measurements.

4. Discussion

[34] By collecting both daytime and nighttime flasks, we were able to characterize isotopic signals associated with net CO_2 exchange and respiratory fluxes. Combining these data with direct eddy flux measurements, we estimated an annual-mean, canopy-scale photosynthetic discrimination

against $^{13}CO_2$. Nonetheless, as we have shown in the sensitivity analyses, calculations of $\delta^{13}C_{bio}$ depend on the quantification of C_{bg} and $\delta^{13}C_{bg}$. The appropriate choice of background air values remains uncertain (here as well as in other studies). Ideally, values of CO_2 mixing ratio and $\delta^{13}CO_2$ from the free atmosphere over regions under investigation are desired. Measurements at a marine station integrate large-scale atmospheric mixing of global CO_2 transport without significant direct impacts from terrestrial ecosystems. The disadvantage of using measurements at a marine station to represent C_{bg} and $\delta^{13}C_{bg}$ for a continental site may involve some lag time that needs to be estimated between the selected station and the investigated site. On the other hand, using smooth curves fitted to local measurements at continental sites to represent C_{bg} and $\delta^{13}C_{bg}$ restricts analyses to processes occurring relatively close to the observing tower [*Miller and Tans*, 2003], and may be more sensitive to uncertainties associated with sampling footprint. The calculated difference in $\delta^{13}C_{bio}$ between the approach used in the current study and that of *Miller et al.* [2003] perhaps indicates a discrepancy in regional footprints of the two approaches.

[35] We can further examine the effect of different $\delta^{13}C_{bio}$ values on the estimated Δ_A for these C_3 forests by once again using Harvard Forest as an example. With $\delta^{13}C_{bio}$ = −24.9‰ as estimated by the approach of *Bakwin et al.* [1998] and *Miller et al.* [2003] (Table 3b) and $\delta^{13}C_R$ = −26.9‰ (Table 2), we calculated $\delta^{13}C_A$ = −26.6‰. This corresponded to Δ_A = 19.1‰, which was "only" 0.5‰ different from our previous approach. Given that errors associated with our experimental approach can be much greater (~ 2‰ as demonstrated in our example), precise determination of $\delta^{13}C_{bio}$ does not guarantee an accurate estimate of Δ_A. Careful flux measurements are also equally important when evaluating Δ_A. It is encouraging that estimates of Δ_A are not hypersensitive to the selection of background air. This +0.5‰ change would have induced a negative atmospheric forcing of $0.5 \times -13 = -6.5$ Mg C ‰ ha^{-1} yr^{-1}. Calculations here reiterated the importance of quantifying temporal and spatial variations in Δ_A. Slight changes in Δ_A can result in large influences on the atmosphere after flux-weighting by one-way gross fluxes, as indicated by the 3.4‰ difference of $\delta^{13}C_{bio}$ between the two different approaches for quantifying C_{bg} and $\delta^{13}C_{bg}$.

[36] To put our observed $\delta^{13}C_{bio}$ in the context of global carbon cycles, Figure 4 shows the latitudinal difference in the estimated $\delta^{13}C_{bio}$ from this study and that of *Miller et al.* [2003]. For references, modeled $\delta^{13}C_A$ from global carbon models of *Fung et al.* [1997], *Lloyd and Farquhar* [1994], *Still et al.* [2003], and Suits et al. (submitted manuscript, 2003) were also shown. Estimates of $\delta^{13}C_{bio}$ at our C_3 forest sites were nowhere close to those at similar latitudes reported by *Miller et al.* [2003]. Such discrepancies may be consequences of different footprints represented by the two analyses. The error bars in our estimates were greater because our sample size was much smaller. Although our data only represented the year between 2001 and 2002 while Miller et al. used data from multiple years, it was the selection of background air that causes the difference between the two studies. We noted that modeled $\delta^{13}C_A$

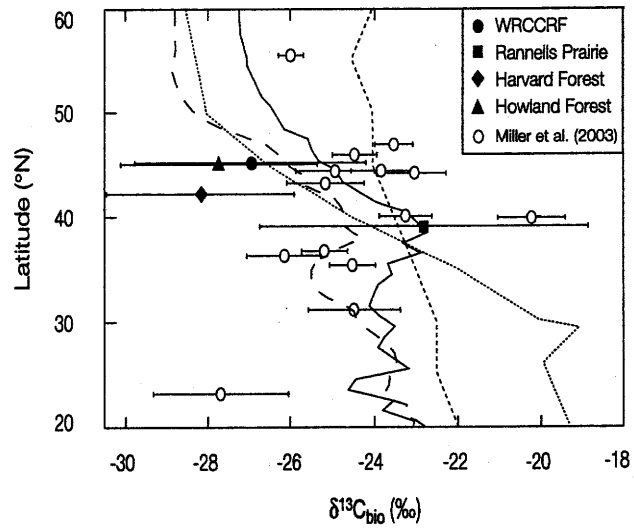

Figure 4. Latitudinal distribution of the annual mean, flux-weighted $\delta^{13}C$ of net ecosystem exchange CO_2 fluxes ($\delta^{13}C_{bio}$). The dash line, dotted line, solid line, and broken line represent modeled $\delta^{13}C_A$ from *Still et al.* [2003], *Fung et al.* [1997], *Lloyd and Farquhar* [1994], and Suits et al. (submitted manuscript, 2003), respectively.

shown in Figure 4 were different from observed $\delta^{13}C_{bio}$. Modeled $\delta^{13}C_A$ represent zonal-mean, flux-weighted values based on relative GPP fluxes of C_3 and C_4 photosynthetic pathways within each latitudinal band. Estimates of $\delta^{13}C_{bio}$ are carbon isotopic compositions of regionally net CO_2 fluxes, representing the balance between GPP and ecosystem respiration. Estimates of $\delta^{13}C_{bio}$ incorporate footprints on the order of several kilometers. We can at best use $\delta^{13}C_{bio}$ as bounds to constrain modeled $\delta^{13}C_A$. For instance, our estimates of $\delta^{13}C_{bio}$ at the C_3 forest sites were more negative than all models, because our isotopic signals were sampled over areas of C_3 vegetation and therefore had no C_4 effect. Modeled $\delta^{13}C_A$ were more positive because GPP of C_4 plants were considered within each latitudinal band. Differences in the modeled latitudinal gradient of terrestrial discrimination were strongly affected by distributions of C_4 photosynthesis. These discrepancies can be reduced with a more recent estimate of the global distribution of C_4 photosynthesis [*Still et al.*, 2003]. One of the unexamined features for the modeling studies shown in Figure 4 is how ecosystem discrimination varies by longitude. As three-dimensional global inversion analyses of CO_2 and $\delta^{13}C$ become available, longitudinal variations of terrestrial ^{13}C discrimination need to be considered as well. Our estimates of $\delta^{13}C_{bio}$ and $\delta^{13}C_R$ at the four ecosystems across the North American continent should also contribute to this developing research area.

[37] Ecosystem ^{13}C signatures (both $\delta^{13}C_R$ and $\delta^{13}C_A$) vary substantially over a growing season and should change from year to year in response to climatic forcing [*Scholze et al.*, 2003]. As the data set grows longer, we can dissect data into seasons to investigate the seasonality of Δ_A or to examine the interannual variability in Δ_A. Long-term and

frequent isotopic air sampling at low latitude, where the contribution of C_4 photosynthesis is relatively high, should be established to validate the modeled gradient in zonal-mean Δ_A [*Lloyd and Farquhar*, 1994; *Fung et al.*, 1997; *Still et al.*, 2003; Suits et al., submitted reference, 2003]. This is particularly important because changes in the proportion of C_3/C_4 distribution would strongly modulate the atmospheric ^{13}C budget. Last, airborne measurements can complement tower-based studies for estimates of C_{bg} and $\delta^{13}C_{bg}$, but are not practical on a routine or continuous basis. For future experimental designs, linking airborne and ground-based experiments would facilitate our understanding of CO_2 exchange between the atmosphere and terrestrial ecosystems.

5. Conclusions

[38] We have shown annual mean ^{13}C signatures associated with canopy gross and net CO_2 fluxes from four sites sampled in the United States. An annual mean, flux-weighted $\delta^{13}C$ of net ecosystem CO_2 fluxes was inferred for C_3 forests and a C_4 prairie. Combining ^{13}C signatures associated with respiratory and net CO_2 fluxes, we demonstrated a measurement-based approach to estimate an annual-mean, canopy-scale photosynthetic discrimination against ^{13}C. The estimated $\delta^{13}C$ ratio associated with photosynthetic fluxes is in agreement with that measured from foliar organic matter. Although the accuracy of our experiment-based analyses is and will continue to be restricted by measurement errors, canopy-scale CO_2 and $\delta^{13}C$ measurements are critical for assessing the validity of modeling studies.

Appendix A: Symbols Used in the Text

- CO carbon monoxide;
- CO_2 carbon dioxide;
- C_{bg} CO_2 mixing ratio of background air (ppm);
- C_{bio} CO_2 mixing ratio associated with biological activities in terrestrial ecosystems (ppm);
- C_{ff} CO_2 mixing ratio associated with fossil fuel combustion (ppm);
- C_m CO_2 mixing ratio within the canopy boundary layer (ppm);
- $\delta^{13}C$ stable carbon isotopic composition (‰);
- $\delta^{14}C$ radioactive carbon isotopic composition (‰);
- $\delta^{18}O$ oxygen isotopic composition (‰);
- $\delta^{13}CO_2$ carbon isotopic composition in CO_2 (‰);
- $\delta^{13}C_A$ carbon isotopic composition associated with gross primary production CO_2 fluxes (‰);
- $\delta^{13}C_{bg}$ carbon isotopic composition in background CO_2 (‰);
- $\delta^{13}C_{bio}$ carbon isotopic composition associated with biological activities in terrestrial ecosystems (‰);
- $\delta^{13}C_{ff}$ carbon isotopic composition associated with fossil fuel combustion (‰);
- $\delta^{13}C_R$ carbon isotopic composition associated with ecosystem respiratory CO_2 fluxes (‰);
- $\overline{\delta^{13}C_R}$ averaged carbon isotopic composition associated with ecosystem respiratory CO_2 fluxes during the growing season (‰);
- $\delta^{13}C_m$ carbon isotopic composition in CO_2 within the canopy boundary layer (‰);
- $\delta^{13}C_{org}$ carbon isotopic composition in leaf organic matter (‰);
- Δ_A whole-canopy photosynthetic discrimination against ^{13}C (‰);
- GPP gross primary production CO_2 fluxes (Mg C ha^{-1} yr^{-1});
- MBL marine boundary layer;
- NEE net ecosystem exchange CO_2 fluxes (Mg C ha^{-1} yr^{-1});
- R ecosystem respiratory CO_2 fluxes (Mg C ha^{-1} yr^{-1});
- $\overline{X}$ bivariate mean of independent variable in the geometric mean regression;
- $\overline{Y}$ bivariate mean of dependent variable in the geometric mean regression.

[39] **Acknowledgments.** We thank the two anonymous reviewers for their constructive comments that have improved this work. We are grateful to Andrew Schauer for his tremendous help on sample collection and analyses. We would like to thank C. Owensby, J. Ham, K. T. Paw, U. D. Shaw, K. Bible, and J. W. Munger for logistic support and data collection. We thank D. Braun, M. Schroeder, L. Auen, B. Hall, and J. Lee for their help with flask collection, and J. Miller and T. Conway for providing the CO_2 and $\delta^{13}CO_2$ data within the NOAA/CMDL network. We are grateful to Edward Peltzer from Monterey Bay Aquarium Research Institute for discussions on Model II statistics. Dan Yakir and Larry Flanagan provide interesting discussions in the early stage of this work. We also thank C. Cook, M. Lott, W. Ike, and B. Dog for assistances on isotope analyses. This research was supported through the Terrestrial Carbon Processes (TCP) program by the office of Science (BER), U.S. Department of Energy under grant DE-FG03-00ER63012.

References

Bakwin, P. S., C. Zhao, W. Ussler III, P. P. Tans, and E. Quesnell (1995), Measurements of carbon dioxide on a very tall tower, *Tellus, Ser. B*, *47*, 535–549.

Bakwin, P. S., P. P. Tans, J. W. C. White, and R. J. Andres (1998), Determination of the isotopic ($^{13}C/^{12}C$) discrimination by terrestrial biology from a global network of observations, *Global Biogeochem. Cycles*, *12*(3), 555–562.

Barford, C. C., S. C. Wofsy, M. L. Goulden, J. W. Munger, E. H. Pyle, S. P. Urbanski, L. Hutyra, S. R. Saleska, D. Fitzjarrald, and K. Moore (2001), Factors controlling long- and short-term sequestration of atmospheric CO_2 in a mid-latitude forest, *Science*, *294*, 1688–1691.

Battle, M., M. L. Bender, P. P. Tans, J. W. C. White, J. E. Ellis, T. Conway, and R. J. Francey (2000), Global carbon sinks and their variability inferred from atmospheric O2 and $\delta^{13}C$, *Science*, *287*, 2467–2470.

Bowling, D. R., P. P. Tans, and R. K. Monson (2001a), Partitioning net ecosystem carbon exchange with isotopic fluxes of CO_2, *Global Change Biol.*, *7*, 127–145.

Bowling, D. R., C. S. Cook, and J. R. Ehleringer (2001b), Technique to measure CO_2 mixing ratio in small flasks with a bellows/IRGA system, *Agric. For. Meteorol.*, *109*, 61–65.

Bowling, D. R., N. G. McDowell, B. J. Bond, B. E. Law, and J. R. Ehleringer (2002), ^{13}C content of ecosystem respiration is linked to precipitation and vapor pressure deficit, *Oecologia*, *131*, 113–124.

Bowling, D. R., D. E. Pataki, and J. R. Ehleringer (2003), Critical evaluation of micrometeorological methods for measuring ecosystem-atmosphere isotopic exchange of CO_2, *Agric. For. Meteorol.*, *116*, 159–179.

Buchmann, N., W. Y. Kao, and J. R. Ehleringer (1997), Influence of stand structure on carbon-13 of vegetation, soils, and canopy air within deciduous and evergreen forests in Utah, United States, *Oecologia*, *110*, 109–119.

Ciais, P., P. P. Tans, M. Trolier, J. W. C. White, and R. J. Francey (1995), A large Northern Hemisphere terrestrial CO_2 sink indicated by the $^{13}C/^{12}C$ ratio of atmospheric CO_2, *Science*, *269*, 1098–1102.

Ciais, P., P. Friedlingstein, D. S. Schimel, and P. P. Tans (1999), A global calculation of the $\delta^{13}C$ of soil respired carbon: Implications for the biospheric uptake of anthropogenic CO_2, *Global Biogeochem. Cycles*, *13*(2), 519–530.

Conte, M. H., and J. C. Weber (2002), Plant biomarkers in aerosols record isotopic discrimination of terrestrial photosynthesis, *Nature*, *417*, 639–641.

Conway, T. J., P. P. Tans, L. S. Waterman, K. W. Thoning, D. R. Kitzis, K. A. Masarie, and N. Zhang (1994), Evidence for interannual variability of the carbon cycle for the National Oceanic and Atmospheric Administration/Climate Monitoring Diagnostics Laboratory Global Air Sampling Network, *J. Geophys. Res.*, *99*, 22,831–22,855.

Ehleringer, J. R., T. E. Cerling, and B. R. Helliker (1997), C4 photosynthesis, atmospheric CO_2 and climate, *Oecologia*, *112*, 285–299.

Ekblad, A., and P. Högberg (2001), Natural abundance of ^{13}C in CO_2 respired from forest soils reveals speed of link between tree photosynthesis and root respiration, *Oecologia*, *127*, 305–308.

Enting, I. G., C. M. Trudinger, and R. J. Francey (1995), A synthesis inversion of the concentration and $\delta^{13}C$ of atmospheric CO_2, *Tellus, Ser. B*, *47*, 35–52.

Farquhar, G. D., J. R. Ehleringer, and K. T. Hubick (1989), Carbon isotope discrimination and photosynthesis, *Annu. Rev. Plant Physiol. Plant Mol. Biol.*, *40*, 503–537.

Fessenden, J. E., and J. R. Ehleringer (2003), Temporal variation in $\delta^{13}C$ of ecosystem respiration in the Pacific Northwest: Links to moisture stress, *Oecologia*, *136*, 129–136.

Flanagan, L. B., and J. R. Ehleringer (1998), Ecosystem-atmosphere CO_2 exchange: Interpreting signals of change using stable isotope ratios, *Trends Ecol. Evol.*, *13*(N1), 10–14.

Flanagan, L. B., J. R. Brooks, G. T. Varney, S. C. Berry, and J. R. Ehleringer (1996), Carbon isotope discrimination during photosynthesis and the isotope ratio of respired CO_2 in boreal ecosystems, *Global Biogeochem. Cycles*, *10*(4), 629–640.

Florkowski, T., A. Korus, J. Miroslaw, J. Necki, R. Neubert, M. Schimdt, and M. Zimnoch (1998), Isotopic composition of CO_2 and CH_4 in a heavily polluted urban atmosphere and in a remote mountain area (Southern Poland), in *Isotope Techniques in the Study of Environmental Change*, pp. 37–48, Int. Atom. Energy Agency, Vienna.

Francey, R. J., P. P. Tans, C. E. Allison, I. G. Enting, J. W. C. White, and M. Trolier (1995), Changes in oceanic and terrestrial carbon uptake since 1982, *Nature*, *373*, 326–330.

Fung, I., et al. (1997), Carbon 13 exchanges between the atmosphere and the biosphere, *Global Biogeochem. Cycles*, *11*(4), 507–533.

GLOBALVIEW-CO2 (2003), Cooperative Atmospheric Data Integration Project: Carbon dioxide [CD-ROM], NOAA Clim. Monit. and Diag. Lab., Boulder, Colo (Available via anonymous FTP to ftp.cmdl.noaa.gov, Path: ccg/co2/GLOBALVIEW).

Högberg, P., A. Nordgren, N. Buchmann, A. F. S. Taylor, A. Ekblad, M. N. Högberg, G. Nyberg, M. Ottosson-Löfvenius, and D. J. Read (2001), Large-scale forest girdling shows that current photosynthesis drives soil respiration, *Nature*, *411*, 789–792.

Keeling, C. D. (1958), The concentrations and isotopic abundances of atmospheric carbon dioxide in rural areas, *Geochim. Cosmochim. Acta*, *13*, 322–334.

Keeling, C. D., S. C. Piper, and M. Heimann (1989), A three-dimensional model of atmospheric CO_2 transport based on observed winds: 4. Mean annual gradients and interannual variations, in *Aspects of Climate Variability in the Pacific and Western Americas*, *Geophys. Monogr. Ser.*, vol. 55, edited by D. H. Peterson, pp. 305–363, AGU, Washington, D. C.

Keeling, C. D., T. P. Whorf, M. Wahlen, and J. van der Plicht (1995), Interannual extremes in the rate of rise of atmospheric carbon dioxide since 1980, *Nature*, *375*, 666–670.

Keeling, C. D., J. F. S. Chin, and T. P. Whorf (1996), Increased activity of northern vegetation inferred from atmospheric CO_2 measurements, *Nature*, *382*, 146–148.

Keeling, C. D., S. C. Piper, R. B. Bacastor, M. Wahlen, T. P. Whorf, M. Heimann, and H. A. Meijer (2001), Exchanges of atmospheric CO_2 and $^{13}CO_2$ with the terrestrial biosphere and oceans from 1978 to 2000: I. Global aspects, *SIO Ref. Ser. 01-06*, pp. 1–45, Scripps Inst. of Oceanogr., San Diego, Calif.

Lai, C.-T., A. J. Schauer, C. Owensby, J. M. Ham, and J. R. Ehleringer (2003), Isotopic air sampling in a tallgrass prairie to partition net ecosystem CO_2 exchange, *J. Geophys. Res.*, *108*, 4566, doi:10.1029/2002JD003369.

Lloyd, J., and G. D. Farquhar (1994), ^{13}C discrimination during CO_2 assimilation by the terrestrial biosphere, *Oecologia*, *99*, 201–215.

Masarie, K. A., and P. P. Tans (1995), Extension and integration of atmospheric carbon dioxide data into a globally consistent measurement record, *J. Geophys. Res.*, *100*, 11,593–11,610.

Meijer, H., H. Smid, E. Perez, and M. Keizer (1997), Isotopic characterisation of anthropogenic CO2 emissions using isotopic and radiocarbon analysis, *Phys. Chem. Earth*, *21*(5–6), 483–487.

Miller, J. B., and P. P. Tans (2003), Calculating isotopic fractionation from atmospheric measurements at various scales, *Tellus, Ser. B*, *55*, 207–214.

Miller, J. B., P. P. Tans, J. W. C. White, T. J. Conway, and B. W. Vaughn (2003), The atmospheric signal of terrestrial carbon isotopic discrimination and its implication for partitioning carbon fluxes, *Tellus, Ser. B*, *55*, 197–206.

Ogée, J., P. Peylin, P. Ciais, T. Bariac, Y. Brunet, P. Berbigier, C. Roche, P. Richard, G. Bardoux, and J.-M. Bonnefond (2003), Partitioning net ecosystem carbon exchange into net assimilation and respiration using $\delta^{13}CO_2$ measurements: A cost-effective sampling strategy, *Global Biogeochem. Cycles*, *17*(2), 1070, doi:10.1029/2002GB001995.

Pataki, D. E., J. R. Ehleringer, L. B. Flanagan, D. Yakir, D. R. Bowling, C. J. Still, N. Buchmann, J. O. Kaplan, and J. A. Berry (2003a), The application and interpretation of Keeling plots in terrestrial carbon cycle research, *Global Biogeochem. Cycles*, *17*(1), 1022, doi:10.1029/2001GB001850.

Pataki, D. E., D. R. Bowling, and J. R. Ehleringer (2003b), Seasonal cycle of carbon dioxide and its isotopic composition in an urban atmosphere: Anthropogenic and biogenic effects, *J. Geophys. Res.*, *108*, 4735, doi:10.1029/2003JD003865.

Potosnak, M. J., S. C. Wofsy, A. S. Denning, T. J. Conway, J. W. Munger, and D. H. Barnes (1999), Influence of biotic exchange and combustion sources on atmospheric CO_2 concentration in New England from observations at a forest flux tower, *J. Geophys. Res.*, *104*, 9561–9569.

Randerson, J. T., G. J. Collatz, J. E. Fessenden, A. D. Munoz, C. J. Still, J. A. Berry, I. Y. Fung, N. Suits, and A. S. Denning (2002), A possible global covariance between terrestrial gross primary production and ^{13}C discrimination: Consequences for the atmospheric ^{13}C budget and its response to ENSO, *Global Biogeochem. Cycles*, *16*(4), 1136, doi:10.1029/2001GB001845.

Rayner, P. J., I. G. Enting, R. J. Francey, and R. Langenfelds (1999), Reconstructing the recent carbon cycle from atmospheric CO_2, $\delta^{13}C$ and O_2/N_2 observations, *Tellus, Ser. B*, *51*, 213–232.

Sage, R. F., D. A. Wedin, and M. Li (1999), The biogeography of C_4 photosynthesis: Patterns and controlling factors, in *C_4 Plant Biology*, edited by R. F. Sage and R. F. Monson, pp. 313–373, Academic, San Diego, Calif.

Schauer, A. J., C.-T. Lai, D. R. Bowling, and J. R. Ehleringer (2003), An automated sampler for collection of atmospheric trace gas samples for stable isotope analyses, *Agric. For. Meteorol.*, *118*, 113–124.

Scholze, M., J. O. Kaplan, W. Knorr, and M. Heimann (2003), Climate and interannual variability of the atmosphere-biosphere $^{13}CO_2$ flux, *Geophys. Res. Lett.*, *30*(2), 1097, doi:10.1029/2002GL015631.

Sokal, R. R., and F. J. Rohlf (1995), *Biometry: The Principles and Practice of Statistics in Biological Research*, W. H. Freeman, N. Y.

Still, C. J., J. A. Berry, G. J. Collatz, and R. S. DeFries (2003), Global distribution of C3 and C4 vegetation: Carbon cycle implications, *Global Biogeochem. Cycles*, *17*(1), 1006, doi:10.1029/2001GB001807.

Suits, N. S., A. S. Denning, J. A. Berry, C. J. Still, J. Kaduk, J. B. Miller, N. Takahashi, H. A. T. Hiyama, E. Konohira, A. Takahashi, N. Yoshida, and T. Nakamura (2001), Balance and behavior of carbon dioxide at an urban forest inferred from the isotopic and meteorological approaches, *Radiocarbon*, *43*(2B), 659–669.

Tans, P. P., J. A. Berry, and R. F. Keeling (1993), Oceanic $^{13}C/^{12}C$ observations: A new window on ocean CO_2 uptake, *Global Biogeochem. Cycles*, *7*(2), 353–368.

Thoning, K. W., and P. P. Tans (1989), Atmospheric carbon dioxide at Mauna Loa observatory: 2. Analysis of the NOAA GMCC Data, 1974–1985, *J. Geophys. Res.*, *94*, 8549–8565.

Trolier, M., J. W. C. White, P. P. Tans, K. A. Masarie, and P. A. Gemery (1996), Monitoring the isotopic composition of atmospheric CO2: Measurements from the NOAA Global Air Sampling Network, *J. Geophys., Res.*, *101*, 25,897–25,916.

Yakir, D., and X.-F. Wang (1996), Fluxes of CO_2 and water between terrestrial vegetation and the atmosphere estimated from isotope measurements, *Nature*, *380*, 515–517.

J. R. Ehleringer and C.-T. Lai, Department of Biology, University of Utah, 257S, 1400E, Salt Lake City, Utah, 84112-0840, USA. (lai@biology.utah.edu)

D. Y. Hollinger, USDA Forest Service, Northeastern Research Station, P.O. Box 640, Durham, NH 03824, USA.

P. Tans, National Oceanic and Atmospheric Administration/Climate Monitoring and Diagnostics Laboratory, 325 Broadway, Boulder, CO 80303, USA.

S. P. Urbanski and S. C. Wofsy, Division of Engineering and Applied Science and Department of Earth and Planetary Science, Harvard University, Cambridge, MA 02138, USA.